Secondary Structure Analysis of Purified Functional CHIP28 Water Channels by CD and FTIR Spectroscopy†

Alfred N. Van Hoek*, Michael Wiener,‡ S. Bicknese, Larry Miercke,‡ Joachim Biwersi, and A. S. Verkman*

Departments of Medicine and Physiology, Cardiovascular Research Institute, and Department of Biochemistry and Biophysics, University of California, San Francisco, California 94143

Received March 5, 1993; Revised Manuscript Received July 2, 1993®

ABSTRACT: The integral membrane protein CHIP28 is an important water channel in erythrocytes and kidney tubule epithelia and is a member of a family of channel/pore proteins including the lens protein MIP26. The purposes of this study were to purify functional, delipidated CHIP28 to homogeneity and to determine secondary structure by circular dichroism (CD) and Fourier transform infrared spectroscopy (FTIR). CHIP28 was initially purified and delipidated by anion-exchange chromatography following solubilization of *N*-lauroylsarcosine-stripped erythrocyte membranes with β-octylglucoside (OG); MIP26 was initially purified and delipidated by anion-exchange chromatography following solubilization of urea-stripped bovine lens membranes by monomyristoylphosphatidylcholine. CHIP28 (glycosylated and nonglycosylated) and MIP26 were purified further by high-performance size-exclusion chromatography, eluting in OG as apparent dimers and tetramers, respectively. Proteoliposomes reconstituted with purified CHIP28 were highly water-permeable, with an osmotic water permeability P_f of 0.04 cm/s at 10 °C that was inhibited by 0.1 mM $HgCl_2$. Proteoliposomes reconstituted with MIP26 had a low P_f of 0.005 cm/s. CD spectra of CHIP28 in OG or in reconstituted proteoliposomes gave a maximum at 193 nm and minima at 208 and 222 nm. Spectral decomposition using protein basis spectra gave 40 ± 5% α-helix and 43 ± 3% β-sheet and -turn. $HgCl_2$ did not affect the CD spectrum of CHIP28. Attenuated total reflectance FTIR of air-dried, membrane-associated CHIP28 gave 38 ± 5% α-helix and 40 ± 4% β-sheet and -turn by spectral decomposition of the amide I resonance. For comparison, CD of MIP26 in OG gave 49 ± 7% α-helix and 32 ± 12% β-sheet and -turn; FTIR gave 32 ± 8% α-helix and 45 ± 6% β-sheet and -turn. Analysis of CHIP28 and MIP26 sequence data by the generalized hydropathy method of Jähnig [Jähnig, F. (1990) *Trends Biochem. Sci. 15,* 93–95] predicted 39–47% α-helix and 15–20% β-structures. These results establish procedures to obtain large quantities of pure CHIP28 and MIP26 in functional forms and provide evidence for multiple membrane-spanning α-helices or mixed α/β-domains.

Fluid absorption and secretion across a number of epithelial and endothelial cell layers involve the osmotically driven movement of water across water-permeable plasma membranes. Biophysical evidence has indicated the existence of specialized "water channels" in plasma membranes in erythrocytes and epithelial cells from mammalian renal tubules and amphibian bladders [for reviews, see Verkman (1992), Finkelstein (1987), and Harris et al. (1991)]. Recently, a cell membrane water channel was isolated and cloned from human erythrocytes (Denker et al., 1988; Smith & Agre, 1991; Preston & Agre, 1991). It is a 28-kDa integral membrane protein (channel-like intrinsic protein, CHIP28) that has 35–45% amino acid homology to the MIP26[1] (major intrinsic protein of lens fiber) family of proteins (Smith & Agre, 1991). Expression of CHIP28 in *Xenopus* oocytes selectively increased water permeability (Preston et al., 1992; Zhang et al., 1993), and reconstitution of CHIP28 in liposomes increased water permeability by >50-fold without affecting urea or proton permeabilities (Van Hoek & Verkman, 1992; Zeidel et al., 1992; Zhang et al., 1993). Antibody localization studies showed that immunoreactive CHIP28 protein is present in renal proximal tubule and thin descending limb of Henle (Sabolic et al., 1992; Nielsen et al., 1993). *In situ* hybridization indicated that mRNA encoding CHIP28 (and/or proteins encoded by homologous mRNAs) is present in these kidney tubule segments as well as in colonic crypt and alveolar epithelial cells, corneal endothelial cells, and other cells associated with physiologically significant water movement (Hasegawa et al., 1993).

The homologous protein MIP26 is thought to facilitate osmotic balance during lens contraction and relaxation. Morphological studies show that MIP26 forms regular orthogonal arrays (Ehring et al., 1990), and it has been proposed that these structures play a role in the communication between adjacent lens fiber membranes. Purified MIP26 forms ion channels when reconstituted into planar bilayers (Ehring et al., 1990; Shen et al., 1991); however, it is not known whether MIP26 is a water transporter.

The secondary structure and membrane topology of CHIP28 and MIP26 are not known. Hydropathy analysis of the predicted amino acid sequence of CHIP28 suggests up to eight

† This work was supported in part by National Institutes of Health Grants DK35124, DK43840, HL42368, and DK16095 to A.S.V. and Grant GM24485 to R. M. Stroud (supporting M.W. and L.M. in carrying out the protein purification), a grant-in-aid from the American Heart Association (A.S.V.), and a grant from the National Cystic Fibrosis Foundation (A.S.V.). M.W. is a Johnson & Johnson Fellow of the Life Sciences Research Foundation. S.B. was supported by NRSA Grant GM15145 and J.B. by a fellowship from the National Cystic Fibrosis Foundation. A.S.V. is an established investigator of the American Heart Association.

* Authors to whom correspondence should be addressed at the Cardiovascular Research Institute.

‡ Department of Biochemistry and Biophysics.

® Abstract published in *Advance ACS Abstracts,* October 15, 1993.

[1] Abbreviations: CHIP28, channel-forming integral protein of 28 kDa; MIP26, major intrinsic lens protein of 26 kDa; HPSEC, high-pressure size-exclusion chromatography; NOD26, soybean nodulin protein; TUR, turgor-response protein of pea shoots; BiB, *Drosophila* big brain protein; GLPF, *E. coli* glycerol facilitator; TIP, tonoplast intrinsic protein; MEMA, putative membrane channel protein of tobacco (RB7-5A).

0006-2960/93/0432-11847$04.00/0

membrane-spanning domains. Biochemical (Smith & Agre, 1991) and morphological (Verbavatz et al., 1993) studies indicate that CHIP28 is assembled as a tetramer in the membrane; however, target analysis studies suggest that the functional unit for water transport is the monomer (Van Hoek et al., 1991). Biochemical studies indicate that the N- and C-termini are oriented cytoplasmically (Smith & Agre, 1991), suggesting that CHIP28 spans the bilayer an even number of times. It is not known whether CHIP28 has the necessary α-helical content to assign multiple α-helical membrane-spanning segments; by analogy to the high-resolution crystal structures of several of the bacterial porins (Weiss et al., 1991; Cowan et al., 1992), CHIP28 may have a β-barrel structure. A mixed α-helix/β-barrel structure is also possible, similar to that predicted by molecular modeling for the voltage-gated Shaker A K^+ channel (Durell & Guy, 1992).

The purposes of this study were to purify and delipidate the CHIP28 and MIP26 proteins in functional forms and to determine secondary structure by circular dichroism (CD) and Fourier transform infrared spectroscopy (FTIR). The functionality of purified CHIP28 was evaluated by water permeability measurements in reconstituted proteoliposomes. Effects of detergent solubilization and mercurial inhibitor binding on CHIP28 secondary structure (α-helix, β-sheet, β-turn, and "other") were determined quantitatively by numerical decomposition of CD and FTIR spectra. The spectral results were then compared to amino acid sequence-based predictions of secondary structure from the analysis of hydropathy, α- and β-amphiphilicity, and β-turn propensity. The data and analyses support the conclusion that CHIP28 and MIP26 contain multiple membrane-spanning α-helical domains.

MATERIALS AND METHODS

Protein Purification

CHIP28. *N*-Lauroylsarcosine-stripped membranes were prepared from human erythrocytes as described previously (Van Hoek & Verkman, 1992). KI-stripped, inside-out erythrocyte vesicles (2 mg of protein/mL) or hemoglobin-free ghosts (5 mg of protein/mL) were treated twice with 3% *N*-lauroylsarcosine in 0.2 mM EDTA and 10 mM sodium phosphate (pH 7.4) (EDTA–phosphate buffer) and centrifuged (300000*g*, Beckman 60 Ti rotor, 60 min, 4 °C). The stripped membranes containing CHIP28 were washed twice with detergent-free buffer and stored on ice at 1 mg of protein/mL (10–15 mg of phospholipid/mL). All subsequent purification was carried out at room temperature unless stated otherwise. Delipidated CHIP28 in detergent micelles was prepared by suspending *N*-lauroylsarcosine-stripped membranes (0.5 mg/mL protein) in EDTA–phosphate buffer containing 200 mM OG (Anatrace Inc., Maumee, OH) for 1 h. The solubilized membranes were filtered through a 0.22-mm disposable filter (Corning, Newark, NJ) and applied to a 2.5 × 5 cm DEAE–Sephacel column (Pharmacia, Rockford, IL) equilibrated in EDTA–phosphate buffer containing 35 mM OG. The eluate was monitored continuously at 280 nm at a flow rate of 0.5 mL/min for sample application and at 1 mL/min for washing and protein elution. After sample application, the matrix was washed with equilibration buffer until the absorbance at 280 nm reached zero, and the protein was eluted with EDTA–phosphate buffer containing 0.6 M NaCl. The DEAE eluate was filtered through a 0.2-μm Acrodisk (Gelman Sciences, Ann Arbor, MI), concentrated using high-pressure ultrafiltration (10-mL Amicon and YM-30 filter, Amicon, Beverly, MA), and applied to a 0.75 × 60 cm TSK G3000SW HPSEC column (Novex Experimental Technology, Encinitas, CA). The column was run in 20 mM sodium phosphate, 100 mM NaCl, and 35 mM OG (pH 7.0) at a flow rate of 0.6 mL/min, and the eluate was monitored at 280 nm.

MIP26. Lens fiber membranes were prepared according to the method of Shen et al. (1991). Frozen mature bovine eyes (Pel-Freeze, Rogers, AR) were thawed and dissected, and 100 lenses were homogenized in 1600 mL of buffer containing 50 mM Tris, 5 mM EDTA, 10 mM DTT, and 20 mg/mL PMSF (pH 7.4). The white turbid homogenate was centrifuged and washed twice (17000*g*, SS34 rotor, 15 min). The membrane pellet (volume, 320 mL) was stripped twice by a 10-min incubation with 7 M urea, 25 mM Tris-HCl, and 20 μg/mL PMSF (pH 7.4), diluted 1:1 with water, centrifuged (27000*g*, SS34 rotor, 20 min), incubated for 10 min with 0.1 N NaOH and 2 μg/mL PMSF, and centrifuged again (44000*g*, SS34 rotor, 20 min). The membranes were dissolved in 20 mM monomyristoylphosphatidylcholine (MMPC, Avanti Polar Lipids Inc., Birmingham, AL) at 0.4 mg/mL for 1 h and subjected to DEAE and size-exclusion chromatography as described for CHIP28, except that both buffers contained 50 mM OG and the mobile phase for size-exclusion chromatography contained 0.6 M NaCl.

SDS–PAGE was performed using a Novex Xcell Mini-Cell electrophoresis system and 4–20% acrylamide/Tris–glycine precast gradient gels. All CHIP28 samples were incubated for 15 min at 60 °C in SDS–PAGE application buffer containing 40 mM DTT; an additional 5% SDS was included with the CHIP28 DEAE and HPSEC samples. MIP26 gel samples were incubated for 2–3 h at room temperature without the inclusion of additional SDS. Gels were stained with Coomassie blue. Total protein concentration was determined by the Lowry assay in the presence of SDS, and lipids were quantified by the phosphorus determination after extraction with chloroform. For Western blotting, proteins were transferred to an immobilon PVDF membrane (Millipore) by electrophoresis at 25 V for 18 h in 10% methanol and 10 mM CAPS (pH 10.4). The membrane was blocked by a 2-h incubation in 150 mM NaCl, 1% Triton X-100, and 20 mM Tris-HCl (pH 7.5) containing 5% (w/w) nonfat milk. The solution was then incubated for 2 h with a 1:500 dilution of rabbit anti-CHIP28 or anti-MIP26 polyclonal antibody (prepared as described in Sabolic et al., 1992), washed, and incubated for 1 h with a goat anti-rabbit IgG horseradish peroxidase-conjugated secondary antibody in the presence of the blocking solution. The blots were washed with 50 mM Tris-HCl (pH 7.5) and assayed for peroxidase activity.

Protein Reconstitution. Lipid vesicles were prepared by reverse-phase evaporation. L-α-Phosphatidylcholine (PC) (400 mg, type V-EA, Sigma), L-α-phosphatidylinositol (PI) (40 mg), and cholesterol (240 mg) (moles of PC:PI:cholesterol = 11:1:11) were dissolved in 1.2 mL of diethyl ether. The solution was hydrated with 3.2 mL of EDTA–phosphate buffer, vortexed vigorously, and evaporated with N_2 to remove the diethyl ether. The milky suspension was dispersed by homogenization in 10 mL of EDTA–phosphate buffer to yield lipid vesicles and then diluted to 100 mL and centrifuged (300000*g*, Beckman 60 Ti rotor, 15 min). The washed vesicles were dispersed in 8.8 mL of the buffer to give 50 mg of phospholipid/mL and were stored on ice.

To reconstitute CHIP28 or MIP26, lipid vesicles were dissolved at 40 °C in EDTA–phosphate buffer containing 150 mM OG, cooled to 20 °C, and mixed with purified OG-solubilized protein. The suspension (lipid/protein = 10 (g/g)) was either dialyzed against detergent-free EDTA–phosphate buffer or slowly diluted with the buffer to decrease

the concentration of OG to 5 mM and centrifuged (300000g, Beckman 60 Ti rotor, 30 min). To remove non-reconstituted protein, the proteoliposome suspension was diluted in 0.5 M sodium phosphate and centrifuged at 300000g for 30 min. A proteoliposome fraction floating on the surface was collected as well as a pellet containing non-reconstituted protein. The proteoliposomes were washed twice with EDTA–phosphate buffer and stored on ice. The protein yield of CHIP28 in proteoliposomes was 50% (MIP26, 33%). The mean vesicle diameter, determined by Coulter counting, was 300 nm for liposomes, 185 nm for CHIP28 proteoliposomes, and 280 nm for MIP26 proteoliposomes.

Permeability Measurements. For the measurement of osmotic water permeability (P_f), vesicles were diluted in EDTA–phosphate buffer and mixed in a stopped-flow apparatus (Hi-Tech SF51, Wiltshire, England) with an equal volume of the buffer containing 200 mM mannitol to produce a 100 mOsm inwardly directed osmotic gradient. Vesicle volume then decreased to ~30% of the initial volume. The time course of decreasing volume was measured by observation of 90° scattered light intensity (520 nm) and was followed until completion using three sequential time scales. In some experiments, membranes were incubated with $HgCl_2$ for 10 min prior to stopped-flow measurement. P_f (cm/s) was determined from the time course of scattered light intensity and vesicle diameter, as described previously (Van Hoek & Verkman, 1992). The single-channel water permeability, p_f (cm^3/s), was calculated from P_f, the lipid-to-protein ratio (L/P, w/w), and the protein density (ρ, 1.35 g/mL) by the equation $p_f = P_f/[(P/L)\rho d N_A/MW]$, where d is membrane thickness (4 nm), N_A is Avogadro's number, and MW is the molecular weight of CHIP28. For the measurement of urea permeability, light scattering was followed after vesicles were subjected to a 100 mM inwardly directed urea gradient.

Circular Dichroism. CD spectra were measured with a Jasco J500A spectropolarimeter (Jasco Inc., Tokyo, Japan). Instrument calibration was carried out using the standard compound (+)-10-camphorsulfonic acid (ratio of ellipticities measured at 192.5 and 290.5 nm was 2.0). Samples were placed in a 0.5 mm path length strain-free quartz cuvette (Helma Cells, Jamaica, NY) that was positioned ~1.5 cm from the photomultiplier (to minimize scattering effects; Dorman et al., 1973). One hundred to two hundred spectra (190–240 nm, 0.2-nm intervals, 1-nm band width) were acquired and averaged (total acquisition time, ~60 min) for each sample.

CD spectra (with base-line spectra subtracted, see below) were converted to molar ellipticity by $[\theta] = (\theta MRW)/(10lc)$ (deg·cm^2/dmol) using the measured ellipticity (θ, deg), protein concentration (c, g/cm^3), cuvette path length (l, 0.05 cm), and mean-residue weight (MRW, 114.3 g/mol). Corrected molar ellipticities at integer wavelengths were used for secondary structure analysis by a least-squares regression (spectral decomposition) using the four-basis spectra set (α-helix, β-sheet, β-turn, and other) of Chang et al. (1978) or the five-basis spectra set ("transmembrane" α-helix, α-helix, β-sheet, β-turn, and other) of Park et al. (1992). The fitted parameters were normalized to report the percentages of each structural form. The absolute molar ellipticities were either floated (unconstrained analysis) or fixed (constrained analysis) in the fitting procedure. The results of all analyses are reported in the Results section. Because of uncertainties in the protein concentration, unconstrained analysis using the Chang et al. (1978) basis set was used to report final secondary structural parameters.

Samples of detergent-solubilized CHIP28 were prepared for CD analysis by desalting the HPSEC-purified proteins (Econo-Pac 10DG desalting column, Bio-Rad, Richmond, CA), followed by dialysis for 2 days at 4 °C against 10 mM sodium phosphate (pH 7) containing 35 mM OG; the protein concentration was adjusted to ~0.1 mg/mL. Samples of detergent-solubilized MIP26 were prepared by dilution of the HPSEC-purified protein or by solubilizing purified lens membranes with 50 mM OG in EDTA–phosphate buffer. The final salt concentration for the HPSEC-purified protein was 100 mM NaCl in 50 mM OG and 10 mM sodium phosphate. In some experiments, reconstituted CHIP28 in proteoliposomes or CHIP28 in lauroylsarcosine-stripped membranes was used; the absorbances of solubilized MIP26 and of membrane-associated CHIP28 were adjusted to ~1.5 at 190 nm (protein concentration, 0.01–0.04 mg/mL). For proteoliposomes, base-line spectra for background subtraction were obtained from samples containing all components except the protein.

Fourier Transform Infrared Spectroscopy (FTIR). Attenuated total reflection Fourier transform infrared (ATR-FTIR) spectroscopy measurements were made on a Nicolet Model 520 FTIR spectrometer (Nicolet Inc., Madison, WI) with a liquid N_2-cooled mercury–cadmium–telluride detector. Measurements were made in the internal reflection mode with an incident beam angle of 45°. Starting samples consisted of stripped erythrocyte or lens fiber membranes or of proteoliposomes containing CHIP28 or MIP26 in 10 mM sodium phosphate (pH 7.4). Samples were prepared by pipeting ~50 μL of protein-containing solution directly onto the surface of a ZnSe window and allowing the sample to dry slowly at room temperature (~45 min). A total of 512 FTIR spectra (1700–400 cm^{-1}, 1.93-cm^{-1} intervals) were acquired and averaged for each sample.

FTIR spectra were analyzed to determine protein secondary structure by the method of Sarver and Krueger (1990). Briefly, the absorbance of the amide I peak (1700–1600 cm^{-1}, vector **a** of length 52) was multiplied by a matrix **F**, which contained the inverse FTIR spectra for pure α-helix, β-sheet, β-turn, and other structures derived by single-value decomposition of the spectra of 17 proteins for which high-resolution crystal structures were available. The product vector **f** = **Fa** contained the contributions from each structural component. The fitted parameters were normalized to report secondary structure percentages.

Secondary Structure Predictions. The primary sequences of CHIP26, MIP26, and six other members of the MIP26 family were analyzed by the generalized hydropathy method of Jähnig (1990). This method combines Kyte–Doolittle hydropathy analysis with Fourier analysis (Finer-Moore & Stroud, 1984) to predict the amphiphilic α-helix and β-sheet content of membrane-associated portions of integral membrane proteins. Briefly, Kyte–Doolittle hydropathy profiles were used first to determine membrane-spanning helical segments. Regions of 20 or more amino acids in the hydropathy profile that had a hydropathy value of greater than 1.6 were assigned as transmembrane helical segments. By extending Jähnig's original formulation, amphiphilic structures of periodicity p were then selected by examination of the "p-weighted" Fourier sum:

$$H(n) = \sum h(n-i)(1 + \cos(2\pi/p))/\sum(1 + \cos(2\pi i/p)) \quad (1)$$

where $H(n)$ is the "p-weighted" hydropathy of residue n, and $h(n)$ is the Kyte–Doolittle hydropathy value of residue n. The

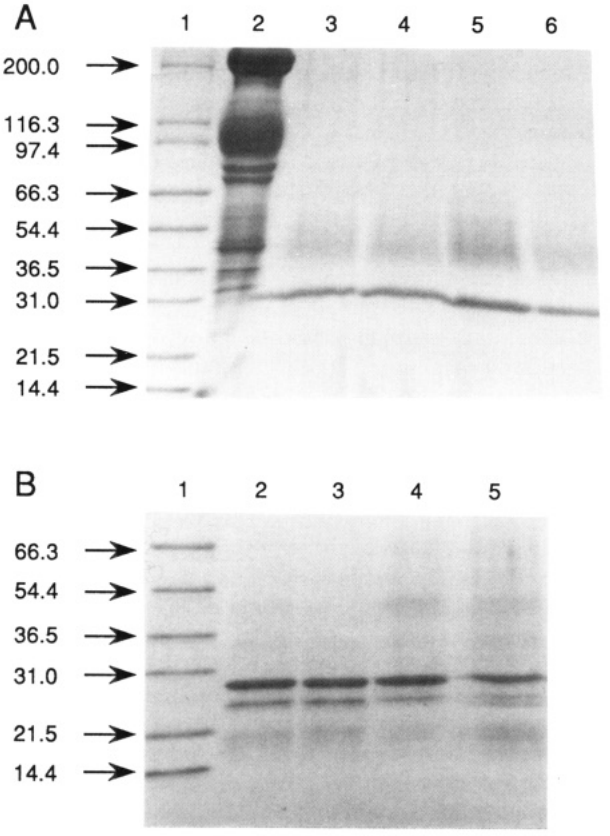

FIGURE 1: SDS–PAGE of CHIP28 and MIP26 samples during the purification procedure. (A) Coomassie blue-stained gel of CHIP28 (see Materials and Methods). Lanes: molecular weight standards (1), erythrocyte ghost membranes (2), OG-solubilized lauroylsarcosine-stripped membranes before (3) and after (4) centrifugation, DEAE-purified CHIP28 (5), and HPSEC-purified CHIP28 (6). (B) Commassie blue-stained gel of MIP26. Lanes: molecular weight standards (1), MMPC-solubilized stripped lens membranes before (2) and after (3) centrifugation, DEAE- (4) and HPSEC-purified (5) MIP26.

sum is taken over residues $i = n-w$ to $n+w$, giving a "window" of width $2w+1$. Values of $p = 3.6$ and 2 were used to detect amphiphilic α-helix and β-sheet, respectively. The hydropathy pattern of an amphiphilic β-sheet will oscillate strongly with frequency (pitch) $p = 2$. According to Jähnig (1990), the minimal and maximal $H(n)$ values should extend beyond the range 0.4–1.6; for $p = 3.6$, the range would be 0.8–1.6. β-turns in connecting loops between transmembrane regions were detected by calculation of the Chou–Fasman turn propensities as described by Jähnig (1990).

RESULTS

Protein Purification and Functional Analysis. Figure 1A shows SDS–PAGE of CHIP28 at various stages of purification. Sequential washing of erythrocyte membranes (lane 2) with KI and *N*-lauroylsarcosine removed nearly all non-CHIP28 proteins (lane 3). CHIP28 stained as a narrow band at ~28 kDa and a broader glycosylated band at an apparent molecular size of 40–55 kDa. Approximately 10–12 mg of protein was isolated from 2 units of human blood (packed cells). CHIP28 was completely solubilized in 200 mM OG (lane 4). Upon DEAE chromatography in OG, there was 80–85% recovery of CHIP28 in detergent micelles (lane 5). CHIP28 was purified by HPSEC (lane 6) with 75% yield; both the 28-kDa (nonglycosylated CHIP28) and 40–55-kDa (glycosylated CHIP28) bands copurified. The overall yield was 3 mg of CHIP28 per unit of blood. Western analysis confirmed that

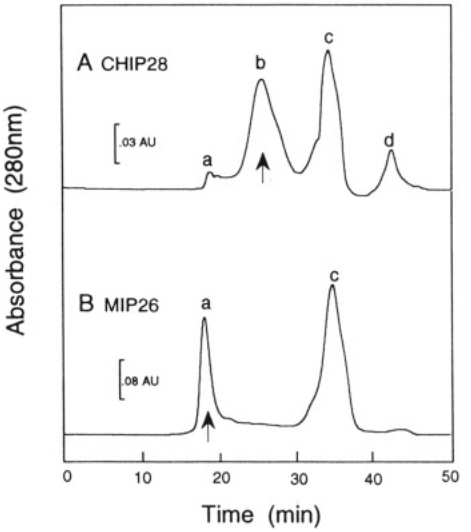

FIGURE 2: HPSEC column elution profile of CHIP28 (A) and MIP26 (B). Chromatography was carried out on a 0.75 × 60 cm TSK G3000SW column using a mobile phase containing OG. The absorbance at 280 nm was followed. Arrows indicate peaks containing purified CHIP28 and MIP26 proteins used for reconstitution and spectroscopy. See the text for details.

both the 28-kDa and 40–55-kDa bands were recognized by the polyclonal anti-CHIP28 antibody (data not shown). The ratio of Commassie staining of the glycosylated to nonglycosylated CHIP28 forms determined by quantitative densitometry was 1–1.1, suggesting that one out of two CHIP28 molecules is glycosylated.

The SDS–PAGE profile of MIP26 during purification steps is shown in Figure 1B. Urea and alkaline washes removed ~99% of total protein (lane 2), yielding 15–25 mg of protein per 25 lenses. A concentration of 20 mM MMPC solubilized >95% of total protein (lane 3). Approximately 45–55% and 35–45% protein were recovered after DEAE (lane 4) and HPSEC (lane 5), respectively, giving a final yield of 3–3.5 mg (16%) of MIP26. The contaminants of lower molecular size (~24 and 20 kDa) were recognized by an anti-MIP26 antibody (data not shown) and are probably proteolytic fragments of MIP26 (Gorin et al., 1984). This purification procedure did not remove the protein contaminants (lanes 3–5), but it did remove nearly all lipid to give a homogeneous MIP26–detergent micelle system.

Figure 2 shows HPSEC elution profiles for DEAE-purified CHIP28 and MIP26. The elution profile for CHIP28 consists of four peaks (from the left): (a) a peak in the void volume containing CHIP28 oligomers; (b) a main peak containing CHIP28 dimers; (c) a peak containing UV-absorbing (primarily non-protein) materials; and (d) a peak arising from the interaction of the injected high-salt OG-solubilized CHIP28 micelles with the low-salt mobile phase. SDS–PAGE, phosphorus assay, and CD analysis of peak c showed small amounts of a ~20-kDa protein (probably a CHIP28 proteolytic fragment), lipids, and cholesterol. CHIP28 (peak b) eluted at an apparent molecular size of 52 kDa [relative to delipidated bacteriorhodopsin (BR), papain-digested BR, and MIP26 (see below)]. This protein was used for subsequent reconstitution and spectroscopic studies. The lipid-to-protein ratio of the final HPSEC-purified CHIP28, measured in a 0.5-mg protein sample, was less than 0.1 (mol/mol), whereas a ratio of 350–400 was measured in the OG-solubilized stripped erythrocyte membranes. The MIP26 elution profile showed a single protein peak (a) with a broad tail and a large lipid/cholesterol peak (c). Peak b was absent, indicating no MIP26

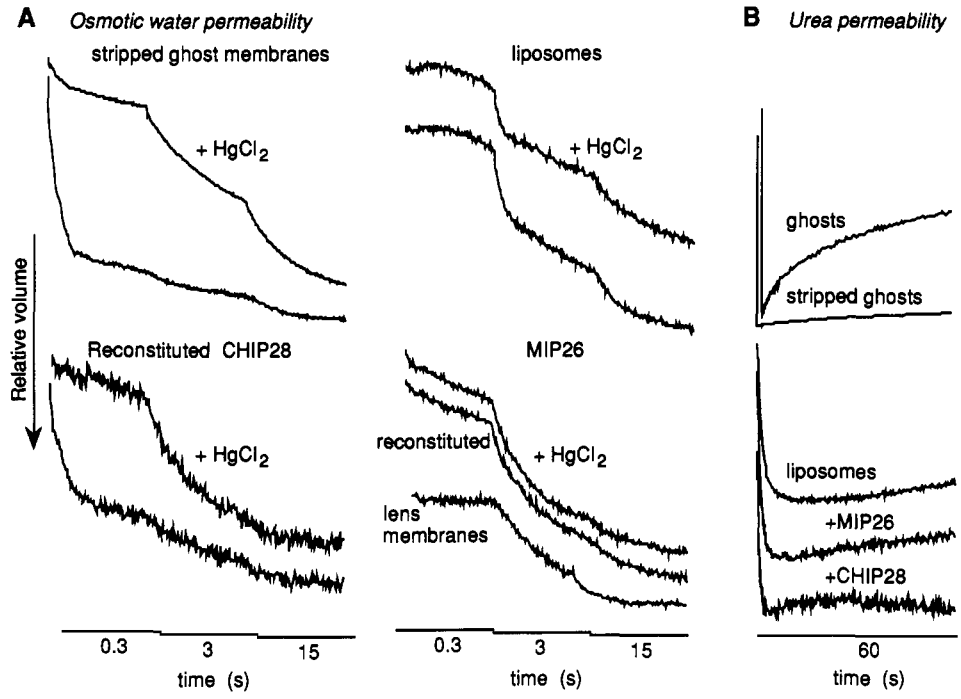

FIGURE 3: Functional analysis of CHIP28 and MIP26. Osmotic water and urea permeability was measured by stopped-flow light scattering at 10 °C. (A) Osmotic water permeability of *N*-lauroylsarcosine-stripped ghost membranes (upper left), (protein-free) liposomes (upper right), and proteoliposomes reconstituted with CHIP28 (lower left) and MIP26 (lower right) in the absence and presence of 0.1 mM $HgCl_2$ and in purified lens membranes (lower right). (B) Urea permeability measured in erythrocyte ghosts before stripping and in the vesicle preparations used in A.

dimers, and peak d was absent because the buffers used for MIP26 purification contained 0.6 M NaCl. The lipid-to-protein ratio for purified MIP was less than 0.1 (mol/mol), as measured in a 0.3-mg protein sample. Whereas CHIP28 eluted mainly as apparent dimers, MIP26 eluted in the void volume as oligomers, probably tetramers of 103 kDa (Aerts et al., 1990) since a TSK 4000 HPSEC chromatogram revealed a single peak (not shown).

Functional analysis of transport was carried out in *N*-lauroylsarcosine-stripped vesicles and proteoliposomes reconstituted with purified CHIP28 and MIP26. Figure 3A shows the time course of vesicle shrinkage in response to an inwardly directed osmotic gradient. *N*-Lauroylsarcosine-stripped ghost membranes, containing mainly CHIP28, retained high water permeability [P_f = 0.013 cm/s, lipid/protein (w/w) = 11.2] that was inhibited by $HgCl_2$ (upper left panel, P_f = 0.0005 cm/s). Proteoliposomes reconstituted with purified CHIP28 also had high water permeability [P_f = 0.042 cm/s, lipid/protein (w/w) = 7.4] that was strongly inhibited by $HgCl_2$ (lower left, P_f = 0.0014 cm/s). The calculated single-channel water permeability (p_f) was $(6 \pm 1) \times 10^{-14}$ cm^3/s at 10 °C (n = 4). Osmotic water permeability in (protein-free) liposomes (upper right, P_f = 0.0035 cm/s) and proteoliposomes reconstituted with MIP26 [lower right, P_f = 0.0045 cm/s, lipid/protein (w/w) = 15.3] was low and insensitive to $HgCl_2$ at concentrations of up to 1 mM. *N*-Lauroylsarcosine-stripped lens membranes (containing MIP26) also had a low osmotic water permeability (lower right) which was $HgCl_2$-insensitive (not shown). An upper limit to the single-channel water permeability for MIP26 was calculated to be 4×10^{-15} cm^3/s. Figure 3B shows the urea permeability as an upward deflection following the initial osmotic shrinkage caused by the inward urea gradient. Whereas urea permeability was rapid in erythrocyte ghost membranes before stripping by *N*-lauroylsarcosine, urea permeability was low after stripping (upper curves) and in the proteoliposomes reconstituted with purified CHIP28 or MIP26 (lower curves). Phloretin (0.2 mM) inhibited urea permeability by >90% in erythrocyte ghost membranes, but had no effect on the time course data for the stripped membranes and reconstituted proteoliposomes (data not shown). These results indicate that CHIP28 is a selective water channel that excludes urea, whereas MIP26 has little water or urea transport activity under the conditions of our experiments.

Spectroscopic Analysis of Secondary Structure. Analysis of CHIP28 secondary structure by CD was performed for CHIP28 in *N*-lauroylsarcosine-stripped erythrocyte membranes, OG detergent micelles, and reconstituted proteoliposomes (Figure 4). The basis spectra sets of Chang et al. (1978) (Figure 4A) and Park et al. (1992) (Figure 4B) were used for decomposition analyses. The Chang et al. basis spectra were derived from linear analysis of the CD spectra from 16 globular proteins with high-resolution crystal structures. The basis spectra of Park et al. were derived from the CD spectra of 30 integral membrane proteins using the convex constraint method of Perczel et al. (1991). The most obvious difference between these two sets are the basis spectra for α-helix and β-turn structures. The Park et al. set contains three basis spectra with similar shapes but different amplitudes, representing α-helix, transmembrane α-helix (α_T), and a type III, class C β-turn as predicted by Woody (1974). The Chang et al. basis set contains a single spectrum for α-helix characteristic of globular proteins; the spectrum for β-turn resembles the type II, class B spectrum predicted by Woody and appears to be the inverse of the Park et al. spectrum for β-turn.

Figure 4C gives the CD spectrum of *N*-lauroylsarcosine-stripped erythrocyte membranes, showing a negative ellipticity with a minimum at ~205 nm. This spectrum could not be analyzed as a linear combination of the protein basis spectra, due to a significant contribution from the abundant lipid and/or cholesterol (10–15 g of lipids/cholesterol per gram of protein) in these preparations. The effect of lipids/cholesterol was tested by measuring the CD spectrum of a solution of

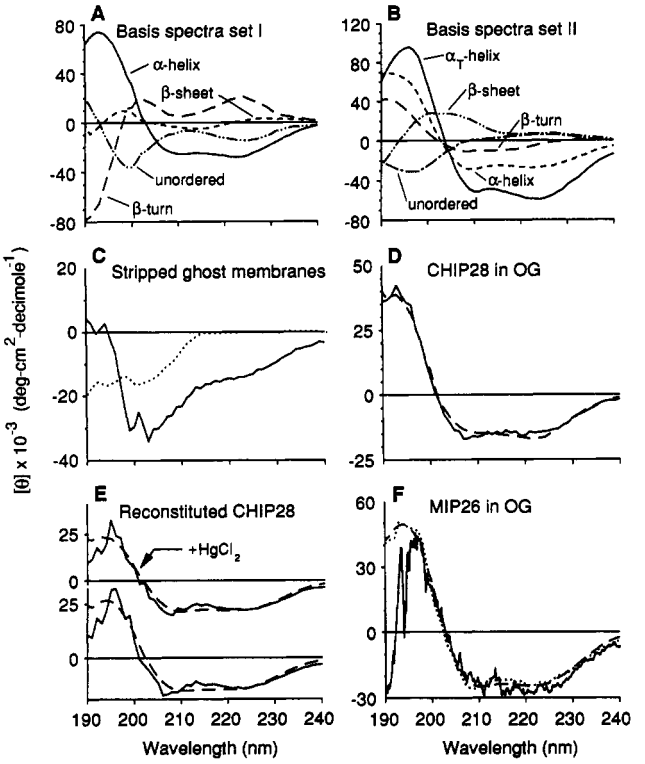

FIGURE 4: CD analysis of CHIP28 and MIP26 secondary structure. (A) Basis spectra of Chang et al. (1978) derived from the CD spectra of 16 globular proteins. (B) Basis spectra of Park et al. (1992) derived from the CD spectra of 30 integral membrane proteins. (C) CD spectra for CHIP28 in lauroylsarcosine-stripped ghost membranes (~0.01 mg/mL, —) and for 1 mM cholesterol in 1 mM PC/0.1 mM PI (···). CD spectra (—) and fitted curves (– –, using Chang et al. basis spectra) of purified CHIP28 (~0.1 mg/mL) solubilized in OG (D), reconstituted CHIP28 (~0.04 mg/mL) in proteoliposomes in the presence and absence of 100 mM $HgCl_2$ (E), and HPSEC-purified MIP26 (0.036 mg/mL, —), and solubilized lens membranes (~0.1 mg/mL, ···) (F). Samples were measured in a 0.05-cm cuvette as described in Materials and Methods. Spectra are averaged, unsmoothed data.

liposomes (1 mM PC and 0.1 mM PI) containing 1 mM cholesterol, which gave a broad minimum from 190 to 205 nm. To test whether high absorption would distort the CD spectrum, *N*-lauroylsarcosine-stripped erythrocyte membranes were mixed with myoglobin. The CD spectra of stripped membranes and of pure myoglobin were independent and additive (not shown). The CD spectrum of purified CHIP28 (Figure 4D) in OG micelles was much different, having a maximum at 193 nm and minima at 208 and 222 nm with a crossover at 201 nm. Subtraction of the liposome/cholesterol spectrum from the stripped erythrocyte membrane spectrum (Figure 4C) produced a CD spectrum that was qualitatively similar to that seen in Figure 4D.

The molar ellipticity at 222 nm for purified CHIP28 in OG corresponded to an α-helical content of 40%. Unconstrained analysis using the Chang et al. basis spectra (see Materials and Methods) gave 42% α-helix, 0% β-turn, 43% β-sheet, and 15% unordered structure. The CD spectrum of reconstituted CHIP28 in proteoliposomes (Figure 4E) gave a pattern similar to that of purified OG-solubilized CHIP28 in the wavelength range 196–240 nm. At shorter wavelengths ($\lambda < 196$ nm), the high absorbance and scattering flattened the CD signal. The molar ellipticity at 222 nm for CHIP28 in proteoliposomes without $HgCl_2$ corresponded to an α-helical content of 43%. Unconstrained analysis (for $\lambda > 195$ nm) using the Chang et al. basis spectra gave 40% α-helix, 15% β-turn, 25% β-sheet, and 20% unordered structure. The same analysis of the CD

Table I: Summary of Secondary Structure Results[a]

	% CHIP28	% MIP26
	CD Analysis	
α-helix	40 ± 5	49 ± 7
β-sheet	42 ± 2	11 ± 7
β-turn	1 ± 2	22 ± 9
other	17 ± 6	18 ± 6
	FTIR Analysis	
α-helix	38 ± 5	32 ± 8
β-sheet	18 ± 2	21 ± 5
β-turn	22 ± 4	24 ± 2
other	22 ± 3	23 ± 2
	Sequence Predictions (Combined for CHIP28 and MIP26)	
α-helix	39–47	
β-sheet	5–9	
β-turn	~10	

[a] Values for CD and FTIR analysis were obtained by spectral decomposition as described in the text. Percentages are mean ± SD for 3–5 separate spectral determinations. Other indicates unordered/random structure and structures otherwise not assigned. Sequence predictions were obtained as described in Materials and Methods and footnote 3. β-turn was estimated by assigning three amino acids to the turn.

spectrum for reconstituted CHIP28 with the addition of 0.1 mM $HgCl_2$ gave 54% α-helix, 5% β-turn, 10% β-sheet, and 31% unordered structure, suggesting no gross change in the secondary structure. For comparison, CD analysis of MIP26 was performed with purified protein and with OG-solubilized purified lens membranes (Figure 4F). The CD spectra of the two preparations showed only small differences except the decrease in the CD signal at $\lambda < 196$ nm for the HPSEC-purified protein, which was due to the presence of 100 mM NaCl. Decomposition using the Chang et al. basis set gave 55% α-helix, 17% β-turn, 10% β-sheet, and 18% unordered structure for MIP26. The averaged fitted values and standard deviations (SD) from multiple independent measurements are summarized in Table I. Qualitatively similar results for the α and β contents were obtained with constrained analysis using the Chang et al. basis spectra and with unconstrained analysis using the Park et al. basis spectra.[2]

Analysis of secondary structure by ATR-FTIR was carried out with CHIP28 and MIP26 in stripped membranes or proteoliposomes using the method of Sarver and Krueger (1990) (see Materials and Methods). Figure 5A shows the basis spectra for α-helix, β-sheet, β-turn, and unordered structure constructed by single-value decomposition of IR spectra in the region of the amide I band from 17 globular proteins. To determine whether secondary structure was influenced strongly by sample dehydration, analysis of the spectrum for myoglobin (Figure 5B) gave an α-helical content consistent with that of the known structure (fitted results: 61% α-helix, 7% β-sheet, 16% β-turn, and 16% unordered structure). The CHIP28 spectrum of stripped ghost mem-

[2] Constrained decomposition of the CD spectrum of purified CHIP28 (Figure 4D) using the Chang et al. basis spectra gave 52% α-helix (α), 31% β-sheet (β-s), no β-turn (β-t), and 18% unordered structure (o) [52 α, 31 β-s, 18 o]; CHIP28 in proteoliposomes (Figure 4E) [51 α, 34 β-s, 15 o]; +$HgCl_2$ [44 α, 31 β-s, 25 o]; MIP26 (Figure 4F) [81 α, 11 β-t, 8 o]. Unconstrained analysis of the purified CHIP28 spectrum using the Park et al. basis gave 2% α_T-helix (α_T), 35% α-helix, 25% β-turn, 6% β-sheet, and 32% unordered structure [2 α_T, 35 α, 25 β-t, 6 β-s, 32 o]; CHIP28 in proteoliposomes [–11 α_T, 55 α, –9 β-t, 6 β-s, 19 o]; +$HgCl_2$ [0 α_T, 57 α, –9 β-t, 3 β-s, 31 o]; MIP26 (Figure 4F) [23 α_T, 16 α, 31 β-t, 4 β-s, 26 o]. Constrained decomposition with the Park et al. five-basis spectra gave two or more negative coefficients for the above spectra, with $\alpha_T < 5\%$. The best constrained fit with positive coefficients (omitting α_T and β-sheet spectra) for purified CHIP28 gave 52% α-helix, 23% β-turn, and 25% unordered structures.

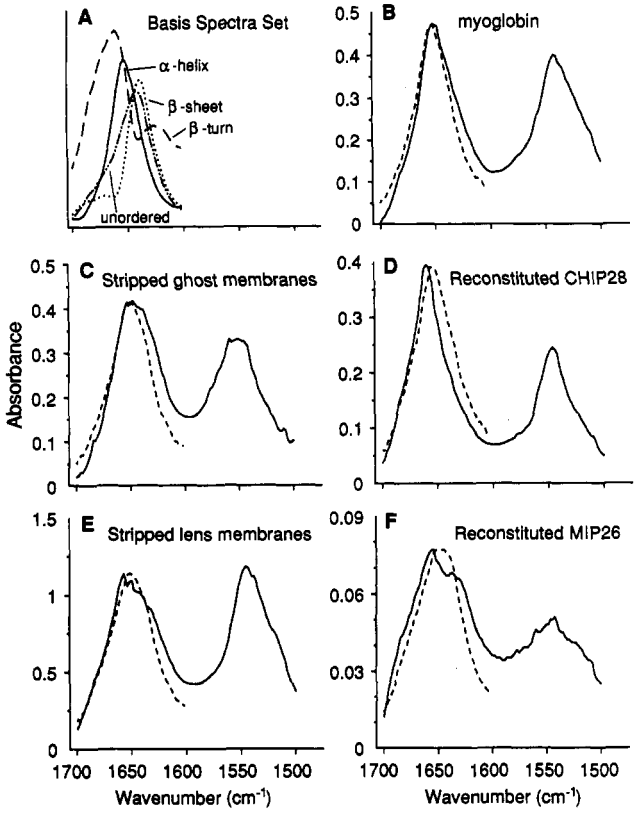

FIGURE 5: FTIR analysis of CHIP28 and MIP26 secondary structure. (A) Basis spectra of Sarver and Krueger (1990) derived from FTIR spectra of 17 globular proteins. FTIR spectra (—) and curve fits (- - -) of myoglobin (~1 mg/mL protein) (B), CHIP28 in *N*-lauroylsarcosine-stripped ghost membranes (~1 mg/mL protein) (C), reconstituted proteoliposomes containing CHIP28 (~1 mg/mL protein) (D), bovine lens membranes containing MIP28 after urea and alkaline stripping (~5 mg/mL protein) (E), and proteoliposomes containing MIP26 (~0.2 mg/mL protein) (F). Samples in 10 mM phosphate buffer were measured as dried films on a ZnSe window as described in Materials and Methods. Spectra are averaged, unsmoothed data.

branes (Figure 5C) had absorbance maxima at 1650 (amide I band) and 1551 cm^{-1} (amide II band). Analysis of the amide I band of CHIP28 gave 46% α-helix, 16% β-turn, 21% β-sheet, and 17% unordered structure. The spectra for proteoliposomes reconstituted with purified CHIP28 (Figure 5D) gave 46% α-helix, 26% β-turn, 2% β-sheet, and 26% unordered structure. The spectrum for MIP26 in stripped lens membranes (Figure 5E) had absorbance maxima at 1658 (amide I band) and 1546 cm^{-1} (amide II band). Spectral analysis gave 35% α-helix, 23% β-turn, 20% β-sheet, and 22% unordered structure; similar spectra were obtained for proteoliposomes reconstituted with purified MIP26 (Figure 5F). The averaged values from several experiments are summarized in Table I.

Secondary Structure Prediction. The secondary structures of CHIP28, MIP26, and six other members of the MIP26 family were predicted by an extension of Jähnig's generalized hydropathy approach (see Materials and Methods). Figure 6 shows the plots generated for CHIP28 and MIP26. Figure 6A is a Kyte–Doolittle hydropathy plot (window width, 7); segments 1, 2, 4–6, and 8 were assigned tentatively as transmembrane helical regions. Figure 6B is an amphipathic profile with periodicity 2, where the first part of segment 2, segment 3, part of segment 5, and segment 6 show strong oscillations and are tentatively assigned as β-strands. Similar analysis with periodicity 3.6 (Figure 6C) suggests that segments 4 and 8 are amphiphilic α-helices. Figure 6D shows the Chou–Fasman prediction for β-turns, which are identified by the maxima in the plot. A similar analysis of secondary structure was carried out for MIP26 (Figure 6E–H). There are eight regions as for CHIP28; however, the assignment of putative amphiphilic β-sheets and α-helices is different. Segment 4 of MIP26 does not show high amplitude with periodicity 2, and segment 1 suggests an amphiphilic α-helix.

To assist in the tentative assignment of secondary structures, the sequences of six other members of the MIP26 family were analyzed separately and then combined by sequence alignment.[3] From hydrophobicity, amphiphilicity, and consensus analyses, segments 1, 2, and 5 were assigned to be hydrophobic α-helices, whereas segment 6 had high hydrophobicity and strong amphiphilicity with periodicity 2, suggestive of a hydrophobic α-helix or β-strand. Segments 4 and 8 were assigned as amphiphilic α-helices. Segment 3, in which one of the highly conserved NPA sequences resides (Wistow et al., 1991), was assigned as an amphiphilic β-sheet, on the basis of periodicity and segment length. Segment 7, in which the other NPA sequence resides, did not show strong periodicity or hydrophobicity and was assigned as β-turn. The Chou–Fasman turn propensity prediction identified the boundaries of segments 1–8 in all members of the MIP26 family. Proteins in the MIP26 family generally contain two halves of similar sequences (Wistow et al., 1991), possibly resulting from the duplication of a common ancestor protein. In the hydropathy profiles for CHIP28 and MIP26, segments 1 and 5, 2 and 6, etc. would resemble each other. However, the analysis suggests that segment 6 is different from segment 2 and that the two NPA consensus sequences (in segments 3 and 7) reside in segments having different secondary structures. The overall percentages of secondary structure elements in CHIP28 and MIP26 are summarized in Table I, and they are in reasonable agreement with the results of CD and FTIR analyses.

DISCUSSION

The primary purpose of this study was to determine the secondary structure of the CHIP28 and MIP26 proteins by spectroscopic methods. The experimental approach involved the purification of these proteins in functional form and the measurement of CD and FTIR spectra. The principal conclusion of this study is that the α-helical contents of CHIP28 and MIP26 are high enough to support predictions, based on the analysis of amino acid sequence, that these proteins contain multiple transmembrane α-helical structures. This conclusion was obtained independently by CD and FTIR spectroscopy with a variety of different protein preparations, including detergent-solubilized protein and membrane-reconstituted protein in suspension or dried to a thin film. The spectroscopic information obtained here establishes a basis for further analysis of protein topology by site-directed insertion of reporter peptides or by construction of chimeras, both of which assume multispanning α-helical motifs; similar analyses of topology have not been attempted for proteins having a transmembrane β-barrel structure or α/β mixed motifs. We note that mixed α/β-domains cannot be ruled out from our data.

[3] The GCG software package (Devereux et al., 1984) was utilized for sequence alignment and analysis. The following members of the MIP26 family were used in sequence alignment: CHIP28, MIP26 (bovine), TUR, MEMA, NOD26, TIP, BIB, and GLPF. Sequences were extracted from the Swissprot database (release 21.0, 3/92) except for TUR [taken from Guerrero et al. (1990)]. Using the aligned sequences, the hydropathy index of each of eight amino acids at position j was averaged to give a series of "consensus" hydropathy plots as in Figure 6. A similar procedure was used for Chou–Fasman analysis of β-turn propensity.

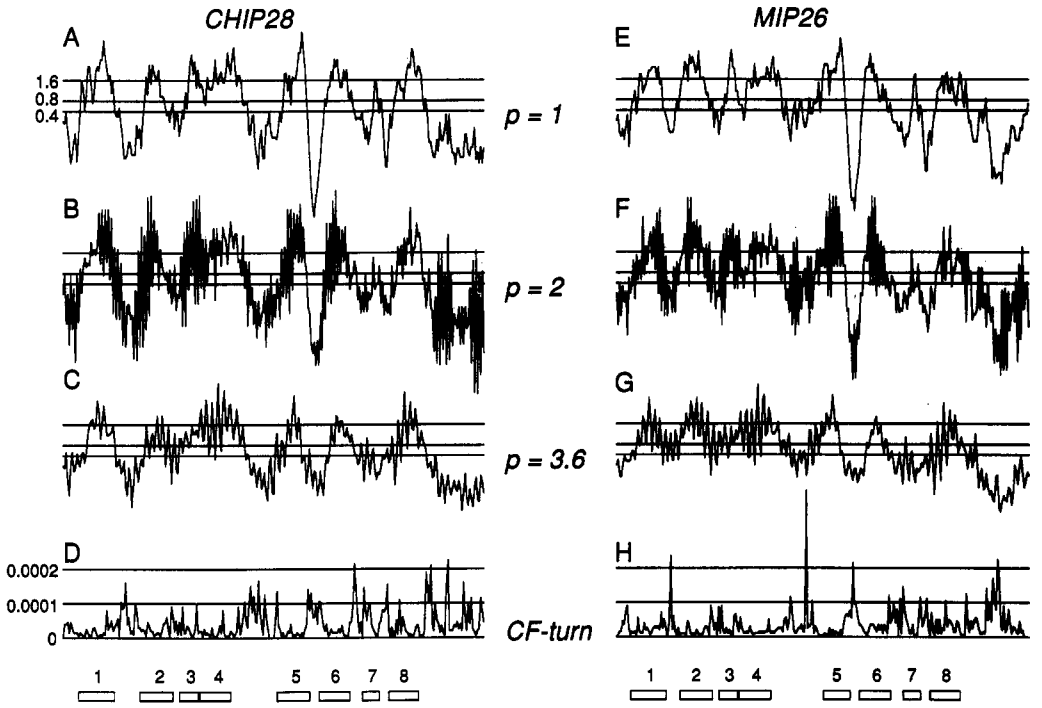

FIGURE 6: Hydropathy and amphipathy plots for CHIP28 (left) and MIP26 (right). (A and E) Hydropathy profiles of Kyte and Doolittle with periodicity 1, window width 7. (B and F) Plots with periodicity 2 and window width 11 to evaluate amphiphilic β-sheet. (C and G) Plots with periodicity 3.6 (see eq 1) and window width 19 to evaluate amphiphilic α-helix. (D and H) Chou–Fasman turn propensity. The horizontal lines in A–C, E, and F represent hydropathy values, $H(n)$, of 1.6, 0.8, and 0.4 (upper to lower) and are used to evaluate hydrophobicity and amphiphilicity as described in Materials and Methods. The horizontal lines in D and H represent probability values.

Size-exclusion and anion-exchange chromatography were combined to prepare purified dimeric CHIP28 in OG from *N*-lauroylsarcosine-stripped erythrocyte membranes, with the removal of nearly all UV-contaminating material. Previously, only anion exchange with Triton X-100 or with Triton X-100 followed by OG was utilized (Denker et al., 1988; Smith & Agre, 1991; Zeidel et al., 1992); CHIP28 yields were not stated, and minor degradation products were present. Purified CHIP28 in OG from size exclusion coupled with anion-exchange chromatography did not contain protein degradation products. This procedure gave a high yield (3 mg/unit of blood) of a mixture of CHIP28 and glycosylated CHIP28 (approximately 1:1) with apparent molecular sizes of 28 and 40–55 kDa on SDS–PAGE.

Delipidated MIP26 was obtained by combining the two chromatographic methods utilized previously for MIP26 purification—size exclusion (Ehring et al., 1990) and anion exchange (Ehring et al., 1991). The yield (1 mg per 3 bovine lenses) was increased substantially by the use of MMPC to solubilize lens membranes. The oligomer population of MIP26 was homogeneous (based on TSK 4000 HPSEC, data not presented) and probably represents MIP26 tetramers (Aerts et al., 1990). Minor contaminants of lower molecular size were present and are believed to represent MIP26 degradation products (Gorin et al., 1984). MIP26 was not glycosylated, and the extent of MIP26 phosphorylation at serines 243 and 245, which can be up to ~20% (Ehring et al., 1991), was not determined. A 3% yield of MIP26 was obtained by size exclusion in OG (Ehring et al., 1990), while incomplete delipidation (10 mol of lipid/mol of MIP26) was produced by DEAE (Ehring et al., 1991; yield not stated). From Figure 2, it is clear that size exclusion should be combined with anion-exchange chromatography to obtain substantially delipidated CHIP28 and MIP26 detergent micelles.

Proteoliposomes reconstituted with purified CHIP28 had high and inhibitor-sensitive osmotic water permeability but low urea permeability, as in (protein-free) liposomes. These results support the conclusion that CHIP28 consists of a narrow pore that is selective for water (Van Hoek & Verkman, 1992; Zeidel et al., 1992). The protein-to-lipid ratio was 0.1 (w/w), which is quite high for reconstitution studies. Functional studies in proteoliposomes and stripped erythrocyte membranes (Figure 3A) suggest that CHIP28 did not lose its water channel function following *N*-lauroylsarcosine stripping, extraction, and solubilization in OG. CD of purified CHIP28 protein and reconstituted protein (Figure 4D,E) revealed no substantial change in secondary structure. The high α-helical content found in CHIP28 (Table I) therefore should be representative of the CHIP28 structure in native erythrocytes. Proteoliposomes reconstituted with purified MIP26 did not have high water permeability and there was no effect of $HgCl_2$. Similar results were obtained in *N*-lauroylsarcosine-stripped purified lens membranes. The protein-to-lipid ratio in the MIP26-containing vesicles was in the same range as that in the CHIP28-containing vesicles. The data suggest that MIP26 obtained by our purification procedure is not a water channel; however, we cannot rule out the possibility that MIP26 may become water-permeable after certain biochemical modifications.

There are a number of methodological concerns in the measurement of CD spectra of membrane proteins, including the validity of background subtraction and the effects of light scattering and absorption. (1) Background subtraction: Ideally the signal arising from background (containing all components except the protein) is nonchiral, so that direct subtraction of the background corrects only for the instrument base line. However, in membrane samples, phospholipids and cholesterol may contribute their own chiral signal to the protein CD spectrum (Chen & Kane, 1986; Figure 4C). Direct subtraction of this lipid background spectrum assumes that the chirality of the lipid components does not change when protein is present. The validity of subtraction of a lipid

background spectrum was examined by resolving a protein–lipid spectrum into a combination of two spectra: lipid/cholesterol and a pure protein (data not shown). For the reconstituted proteoliposomes containing CHIP28 used in our study, the lipid and protein CD spectra were nearly independent and additive. (2) Light scattering: Light scattering by macromolecules and lipid–protein complexes can alter the CD spectrum from a protein and/or add spurious signals from circular intensity differential scattering (CIDS). CIDS results from the differential scattering of right and left circularly polarized light and thus has greatest effects at shorter wavelengths. Possible scattering artifacts were minimized by positioning the thin cuvette ~1.5 cm from the photomultiplier surface to capture the scattered light. Increasing the cuvette-detector distance to 5 cm had little effect on CD spectra, indicating little or no scattering effects. (3) Light absorption: Gordon and Holzwarth (1971) reported absorption flattening of CD spectra leading to erroneous structural analysis for proteins in membrane suspensions where the absorbing chromophores are not distributed uniformly (Duysens effect). The similar structural results for the analysis of CD spectra measured in detergent-solubilized CHIP28 and in reconstituted proteoliposomes suggest that the Duysens effect was not significant in our measurements.

Several methods have been used for secondary structure determinations using protein CD spectra. Helical content has been estimated directly from molar ellipticity at 222 nm, whereas analysis of protein structure in terms of fractions of α-helix, β-sheet, β-turn, and other structures has been obtained by decomposing the measured CD spectrum in terms of a set of basis spectra representing the four individual (and assumed independent) secondary structures. The four-basis spectra of Chang et al. (1978) (51×4 matrix **S**) were calculated by linear solution of the equation $\mathbf{R} = \mathbf{SF}$, where **R** is a 51×16 matrix containing the CD spectra for 16 globular proteins, and **F** is a 4×16 matrix derived from high-resolution crystal structure data for the individual secondary structures (α-helix, β-sheet, β-turn, and other) of the proteins. It should be noted that these basis spectra were derived from data obtained on soluble proteins, so that analyses of spectra for membrane proteins must be interpreted with caution. The five-basis spectra of Park et al. (1992) were derived from the CD spectra of 30 membrane proteins (Figure 4B). Each basis spectrum was attributed to a specific protein secondary structure on the basis of its similarity to a CD basis spectrum predicted by theory and/or found in other basis sets.

The most significant differences between the two basis sets used here (Park et al. and Chang et al.) are the spectra for α-helices and β-turns. The Park et al. basis set contains two helix-type spectra and designates the one with greater amplitude as a transmembrane α-helix. This is primarily because the 20-residue helix needed to span the membrane is expected to have a stronger CD signal than the average helix found in globular proteins (10 residues) (Chang et al., 1978). The spectra for β-turns differed substantially in the two basis sets. The β-turn represented in the Chang et al. basis set is predicted to be the most common among proteins (Woody, 1974), whereas that of Park et al. may be typical among membrane-associated proteins. The Park et al. basis spectra were expected to be appropriate for analysis of the membrane-associated CHIP28 and MIP26 proteins; however, all analyses carried out with this basis set produced one or more negative coefficients.[2] The similarity of three Park et al. basis spectra (α_T-helix, α-helix, and β-turn) make the analysis sensitive to small variations in spectral shape. Such variations could arise from changes in tertiary structure (see below) and slight flattening of the CD spectra by scattering and ion absorption. We have thus reported the results in Table I using the Chang et al. basis set.

Another concern is that the CD spectrum is not sensitive to protein secondary structure exclusively; even globular proteins have significant variations in CD spectral shape with tertiary structure (Parthasarathy & Johnson, 1983), content of aromatic side chains (Woody, 1978), and disulfide bonds (Perczel et al., 1991). The CD spectra of proteins containing α and β structures usually contain negative ellipticity minima at 208 and 222 nm. Parthasarathy and Johnson (1983) showed that the 222-nm peak has the greater magnitude in proteins where the α- and β-domains are mixed, whereas the 208-nm peak has the greater magnitude in proteins where the α- and β-domains are separate. The 208-nm peak has the greater magnitude in the CD spectra of CHIP28 and MIP26 (Figure 4D–F), suggesting that the α and β structures of these membrane proteins are in separate domains. In addition, the positions of the peaks in CD spectra for membrane proteins are slightly different from those for water-soluble proteins (Park et al., 1992). Given these caveats, the CD results were compared with those obtained by an independent experimental approach involving infrared spectroscopy, as well as secondary structure prediction from primary sequence information.

Infrared spectroscopy provides information about protein secondary structure from the spectral shape and position of the amide I and II peaks. FTIR and CD spectroscopy are complementary methods of structural analysis because they are subject to different potential sources of error (Surewicz et al., 1993). The details of the amide peaks are determined by differences in hydrogen bonding associated with α-helix, β-sheet, β-turn, and "other" structures. Measurement of ATR-FTIR spectra required drying of the samples to a thin film in order to minimize the absorbance of infrared light by water. The relative dehydration of samples studied by FTIR can, in principle, alter protein structure and create difficulty in the preparation of samples suitable for background subtraction. However, our analysis of the secondary structures of pure, dried proteins [myoglobin (Figure 5B), lysozyme, bacteriorhodopsin, and elastase, data not shown] agreed well with that reported by Kabsch and Sander (1983). The spectra of dried background samples containing lipid alone had no absorption peaks in the amide I and II regions, so that their subtraction provided little correction to spectral shape.

The analysis of protein secondary structure from the FTIR amide I peak was accomplished by the matrix multiplication method of Sarver and Krueger (1990). The alternative method of Venyaminov and Kalnin (1990) makes use of three basis spectra, each containing spectral information about both the amide I and II peaks, derived from FTIR spectra of polypeptides with assumed uniform secondary structures (α-helix, β-sheet, and random coil). Analysis of FTIR spectra for CHIP28 and MIP26 by this method did not distinguish between α-helices and random coil, giving fitted percentages as high as 90% for random coil (results not shown). Analysis methods involving band narrowing and Fourier spectral deconvolution were considered (Surewicz et al., 1993). These methods are, in general, very sensitive to experimental noise and lack unique solutions because of the large number of fitted parameters required to describe multiple spectral peaks.

The method of Sarver and Krueger (1990) appeared to be superior for the resolution of different structural forms. They report that spectral decomposition using only the amide I peak correlated better with X-ray structural data than results

using both the amide I and II peaks. Their basis spectra were derived from globular proteins containing a mixture of structural forms, rather than from simple polypeptides with assumed uniform structure. It is recognized that the analysis of CHIP28 or MIP26 secondary structure by either of these methods may be subject to systematic errors because the basis spectra were obtained using water-soluble globular proteins. The α-helical contents in CHIP28 and MIP26 determined by FTIR are smaller than, but in reasonable agreement with, those obtained by CD analysis. It is generally thought that CD is superior for identification of the helix structure, whereas FTIR is better for β-sheet (Sarver & Krueger, 1990). When β-sheet and -turn are summed together as β-structures, then CD and FTIR analyses give similar results.

Secondary structure was predicted from sequence data using Kyte–Doolittle hydropathy profiles, Fourier analysis of periodicity, and Chou–Fasman analysis of β-turn propensity. The assignment of secondary structures was facilitated by sequence alignment of eight members of the MIP26 family of proteins as described in footnote 3. The percentage of predicted α-helix (hydrophobic + amphiphilic) was in reasonable agreement with CD and FTIR analyses of secondary structure. The percentage of predicted β-sheet represents a minimum value because only amphiphilic strands were predicted from the length of the segment and the magnitude of the oscillations in hydropathy profiles of periodicity 2.

ACKNOWLEDGMENT

We thank Dr. R. M. Stroud for scientific advice and support throughout the project, Dr. J. T. Yang for advice on the analysis of CD and FTIR spectra, Dr. G. Fasman for generously providing the convex constraint analysis software, and Dr. R. Sarver for advice on the analysis of FTIR spectra.

REFERENCES

Aerts, T., Xia, J. Z., Slegers, H., de Block, J., & Clauwaert, J. (1990) *J. Biol. Chem. 265*, 8675–8680.

Chang, C. T., Wu, C. C., & Yang, J. T. (1978) *Anal. Biochem. 91*, 13–31.

Chen, C. C., & Kane, J. (1986) *Methods Enzymol. 128*, 519–527.

Cowan, S. W., Schirmer, T., Rummel, G., Steiert, M. Ghosh, R., Pauptit, R. A., Jansenius, J. N., & Rosenbusch, J. P. (1992) *Nature 358*, 727–733.

Denker, B. M., Smith, B. L., Kuhajda, F. P., & Agre, P. (1988) *J. Biol. Chem. 263*, 15634–15642.

Devereux, H., Haeberi, L. P., & Smithies, O. (1984) *Nucleic Acids Res. 12*, 387–395.

Dorman, B., Hearst, J. E., & Maestre, M. F. (1973) *Methods Enzymol. 25*, 767–796.

Durell, S. R., & Guy, H. R. (1992) *Biophys. J. 62*, 238–250.

Ehring, G. R., Zampighi, G., Horwitz, J., Bok, D., & Hall, J. E. (1990) *J. Gen. Physiol. 96*, 631–664.

Ehring, G. R., Lagos, N., Zampighi, G. A., & Hall, J. E. (1991) *J. Membr. Biol. 126*, 75–88.

Finer-Moore, J., & Stroud, R. M. (1984) *Proc. Natl. Acad. Sci. U.S.A. 81*, 155–159.

Finkelstein, A. (1987) Water movement through lipid bilayers, pores, and plasma membranes, in *Distinguished Lecture Series of the Society of General Physiologists*, Wiley-Interscience, New York.

Gordon, D. J., & Holzwarth, G. (1971) *Arch. Biochem. Biophys. 142*, 481–488.

Gorin, M. B., Yancey, S. B., Cline, J., Revel, J. P., & Horwitz, J. (1984) *Cell 39*, 49–59.

Guerrero, F. D., Jones, J. T., & Mullet, J. E. (1990) *Plant Mol. Biol. 15*, 11–26.

Harris, H. W., Strange, K., & Zeidel, M. (1991) *J. Clin. Invest. 91*, 1–8.

Hasegawa, H., Zhang, R., Dohrman, A., & Verkman, A. S. (1993) *Am. J. Physiol. 264*, C237–C245.

Jähnig, F. (1990) *Trends Biochem. Sci. 15*, 93–95.

Kabsch, W., & Sander, C. (1983) *Biopolymers 22*, 2577–2639.

Nielsen, S., Smith, B. L., Christensen, E. I., Knepper, M. A., & Agre, P. (1993) *J. Cell Biol. 120*, 371–383.

Park, K., Perczel, A., & Fasman, G. (1992) *Protein Sci. 1*, 1032–1049.

Parthasarathy, M., & Johnson, W. C. (1983) *Nature 305*, 831–832.

Perczel, A., Hollo, M. Tusnð, G., & Fasman, G. (1991) *Protein Eng. 4*, 669–679.

Preston, G. M., & Agre, P. (1991) *Proc. Natl. Acad. Sci. U.S.A. 88*, 11110–11114.

Preston, B. M., Carroll, T. P., Guggino, W. B., & Agre, P. (1992) *Science 256*, 385–387.

Sabolic, I., Valenti, G., Verbavatz, J. M., Van Hoek, A. N., Verkman, A. S., Ausiello, D.A., & Brown, D. (1992) *Am. J. Physiol. 263*, C1225–C1233.

Sarver, R. W., & Krueger, W. (1990) *Anal. Biochem. 194*, 89–100.

Shen, L., Shrager, P., Girsch, S. J., Donaldson, P. J., & Peracchia, C. (1991) *J. Mol. Biol. 124*, 21–32.

Smith, B. L., & Agre, P. (1991) *J. Biol. Chem. 266*, 6407–6415.

Surewicz, W. K., Mantsch, H. H., & Chapman, D. (1993) *Biochemistry 32*, 389–394.

Van Hoek, A. N., & Verkman, A. S. (1992) *J. Biol. Chem. 267*, 18267–18269.

Van Hoek, A. N., Hom, M. L., Luthjens, L. H., De Jong, M. D., Dempster, J. A., & Van Os, C. H. (1991) *J. Biol. Chem. 226*, 16633–16635.

Venyaminov, S. Y., & Kalnin, N. N. (1990) *Biopolymers 30*, 1259–1271.

Verbavatz, J. M., Brown, D., Sabolic, I., Valenti, G., Van Hoek, A. N., Ma, T., & Verkman, A. S. (1993) *J. Cell Biol.*, (in press).

Verkman, A. S. (1992) *Annu. Rev. Physiol. 54*, 97–108.

Weiss, M. A., Abele, U., Weckesser, J., Welte, W., Schiltz, E., & Schulz, G. E. (1991) *Science 254*, 1627–1630.

Wistow, G. J., Pisano, M. M., & Chepelinsky, A. B. (1991) *Trends Biochem. Sci. 16*, 170–171.

Woody, R. W. (1974) In *Peptides, Polypeptides and Proteins* (Blout, E. R., Bovey, F. A., Goodman, M., & Lotan, N., Eds.) pp 338–350, John Wiley & Sons, New York.

Woody, R. W. (1978) *Biopolymers 17*, 1452–14757.

Zeidel, M. L., Ambudkar, S. V., Smith, B. L., & Agre, P. (1992) *Biochemistry 31*, 7436–7440.

Zhang, R., Skach, W., Hasegawa, H., Van Hoek, A. N., & Verkman, A. S. (1993) *J. Cell Biol. 120*, 359–369.